Supplementary Information for

Molecular mechanism of substrate recognition by folate transporter SLC19A1

Authors:

Yu Dang[1], Dong Zhou[2], Xiaojuan Du[3]†, Hongtu Zhao[4], Chia-Hsueh Lee[4], Jing Yang[3], Yijie Wang[3], Changdong Qin[5], Zhenxi Guo[5], and Zhe Zhang[1,2,3*]

Affiliations:

[1]State Key Laboratory of Membrane Biology, Peking University-Tsinghua University-National Institute of Biological Sciences Joint Graduate Program, Academy for Advanced Interdisciplinary Studies, Peking University, Beijing 100871, China

[2]Center for Life Sciences, Academy for Advanced Interdisciplinary Studies, Peking University, Beijing 100871, China

[3]School of Life Sciences, Peking University, Beijing 100871, China

[4]Department of Structural Biology, St. Jude Children's Research Hospital, Memphis, TN 38105, United States

[5]Cryo-EM Platform, School of Life Sciences, Peking University, Beijing 100871, China

†Present address: Peking University First Hospital, Peking University Health Science Center, Beijing 100191, China

[*]Correspondence should be addressed to zzhang01@pku.edu.cn.

This file includes:

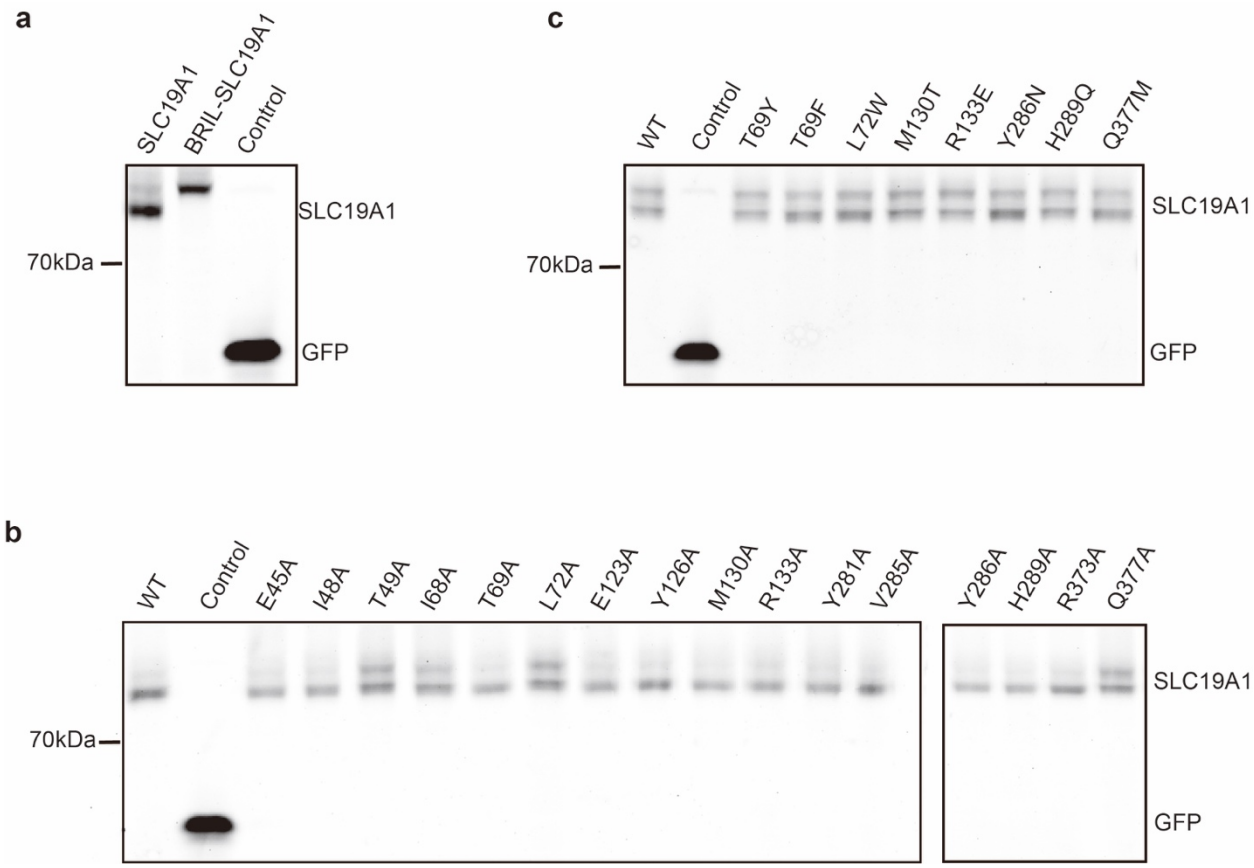

Supplementary Fig. S1 Detection of the SLC19A1 expression by SDS-PAGE.

a-c Verification of the expression level of different SLC19A1 variants or mutants for the [^{3}H]-MTX uptake assays using the GFP fluorescence signal. All experiments were repeated three times with similar results.

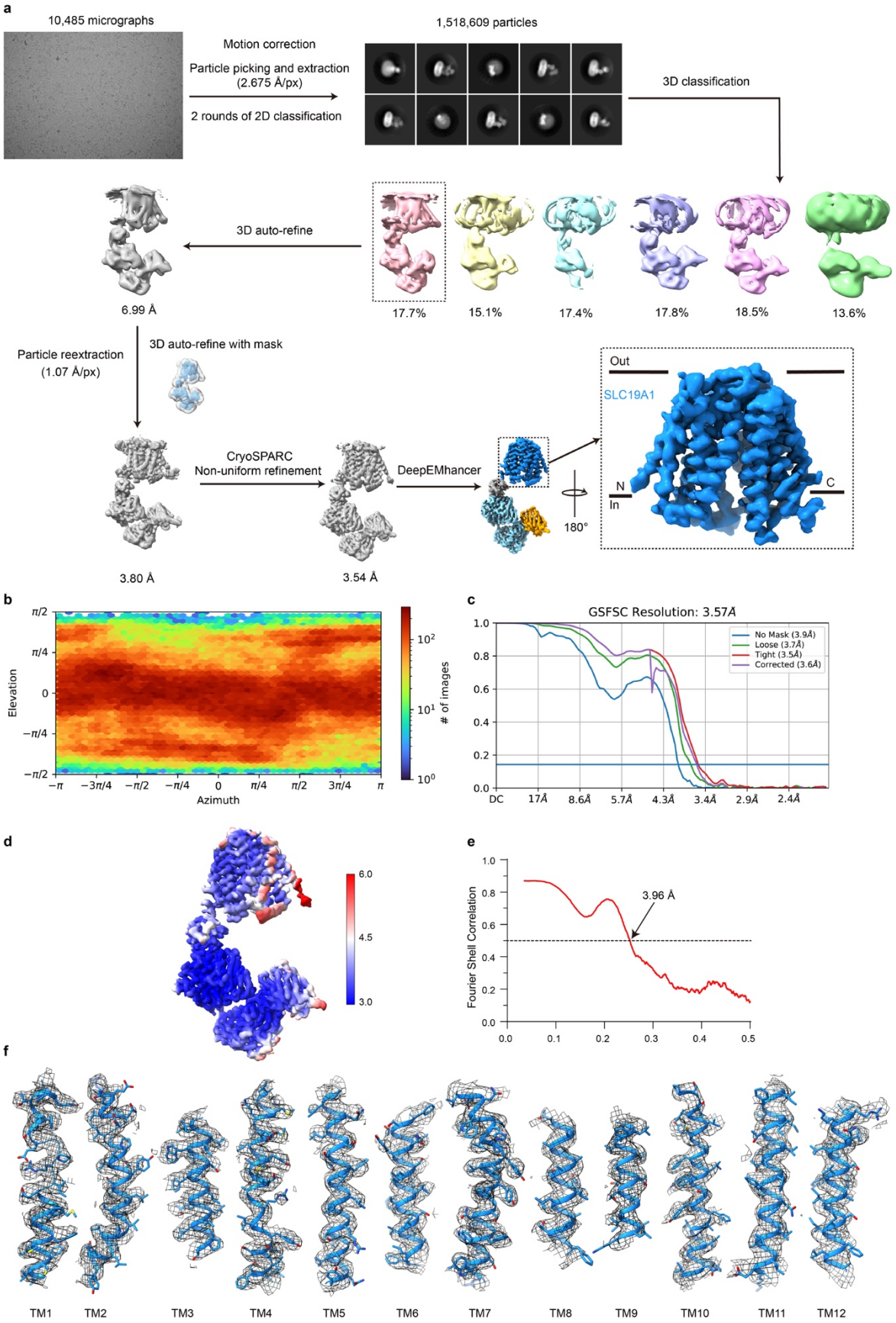
a
10,485 micrographs
Motion correction
Particle picking and extraction
(2.675 Å/px)
2 rounds of 2D classification
1,518,609 particles
3D classification
17.7%
15.1%
17.4%
17.8%
18.5%
13.6%
3D auto-refine
6.99 Å
Particle reextraction
(1.07 Å/px)
3D auto-refine with mask
CryoSPARC
Non-uniform refinement
3.80 Å
3.54 Å
DeepEMhancer
180°
Out
SLC19A1
N
In
C
b
Elevation
Azimuth
# of images
c
GSFSC Resolution: 3.57Å
No Mask (3.9Å)
Loose (3.7Å)
Tight (3.5Å)
Corrected (3.6Å)
d
e
Fourier Shell Correlation
3.96 Å
f
TM1
TM2
TM3
TM4
TM5
TM6
TM7
TM8
TM9
TM10
TM11
TM12

Supplementary Fig. S2 Cryo-EM data processing of the apo SLC19A1 dataset.

a Work flow of the data processing. **b** Orientation distribution of the particles used in final reconstruction. **c** Fourier shell correlation (FSC) curves between two half maps. **d** Local resolution of the cryo-EM map. **e** FSC curve calculated between cryo-EM map and structural model. **f** Close-up view of the cryo-EM densities and fitted atomic models for representative regions of the structure.

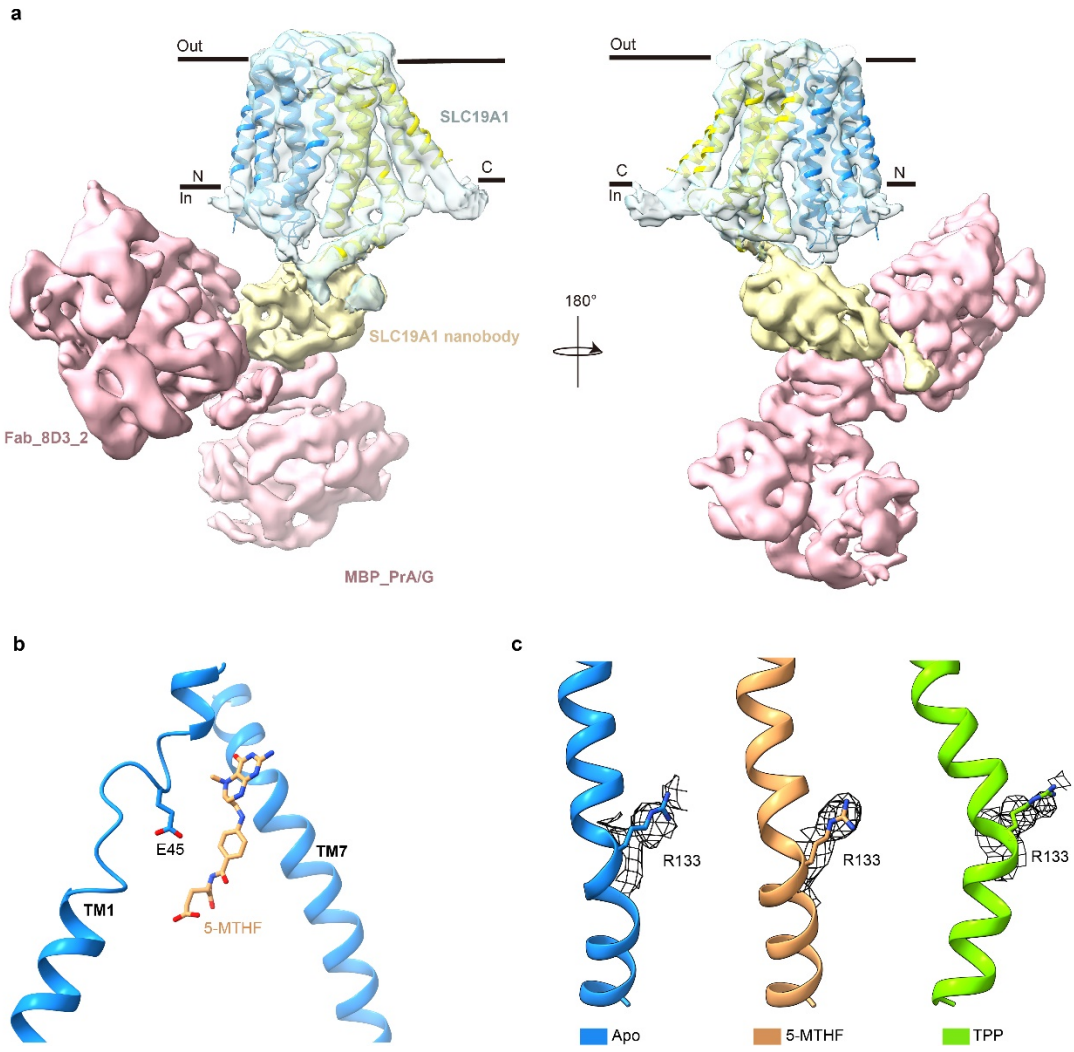

Supplementary Fig. S3 Structure analyses of SLC19A1.

a Cryo-EM map of the SLC19A1/legobody complex shown in two views. The structure model of SLC19A1 can be fitted well into the EM map. The two half TM bundles of SLC19A1 are colored in blue (TM1-6) and yellow (TM7-12), respectively. The maps of SLC19A1, SLC19A1 nanobody, and the other two components of legobody (MBP_PrA/G and Fab_8D3_2) are colored in light blue, wheat, and pink, respectively. **b** Location of Glu45 in the structure of the SLC19A1/5-MTHF complex. TM1 and TM7 are shown as ribbon. 5-MTHF and the side chain of Glu45 are indicated as sticks. **c** Cryo-EM densities of Arg133 in the three SLC19A1 structures. The side chains of Arg133 are shown as sticks and the cryo-EM densities are shown as black meshes.

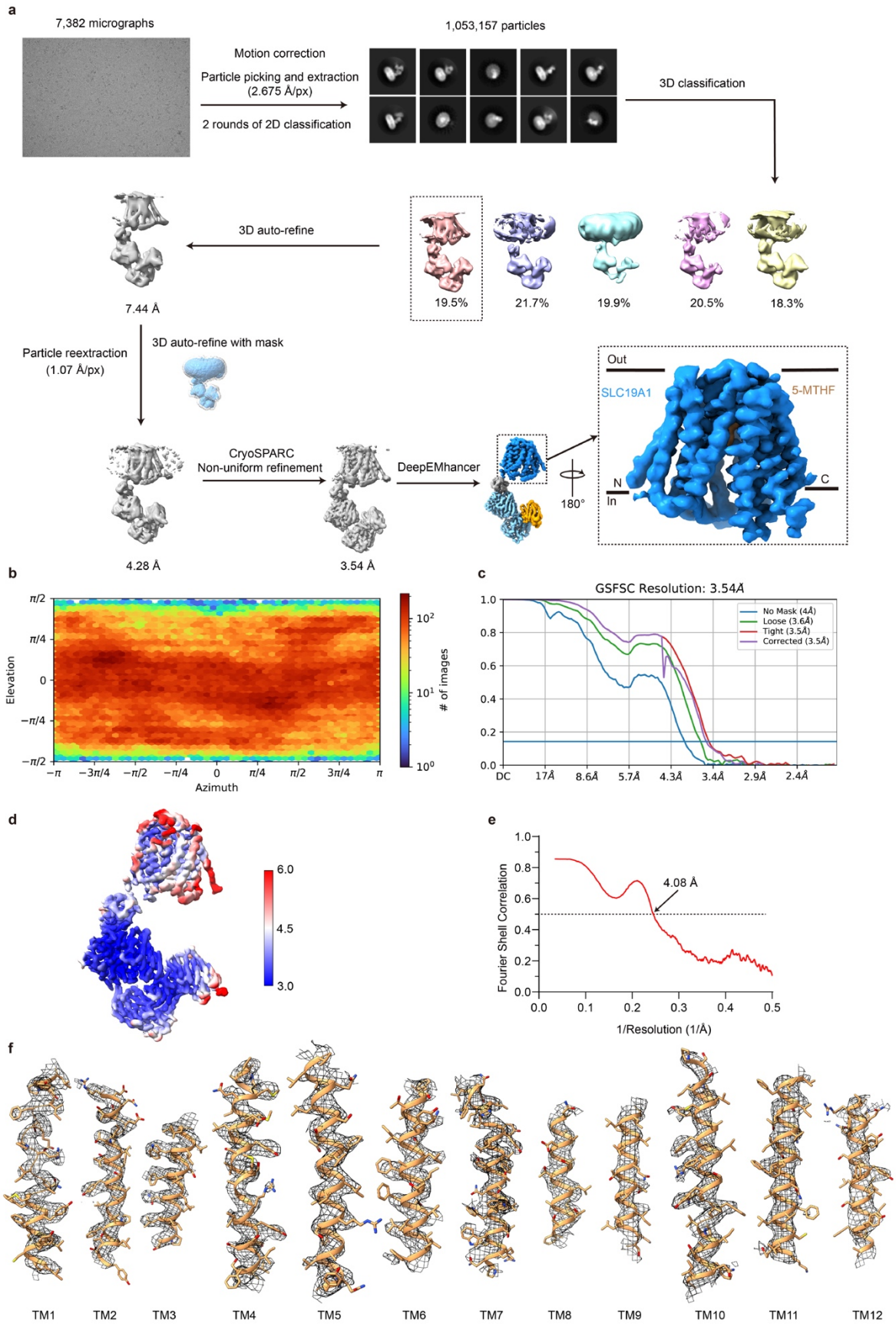
a
7,382 micrographs
Motion correction
Particle picking and extraction
(2.675 Å/px)
2 rounds of 2D classification
1,053,157 particles
3D classification
19.5%
21.7%
19.9%
20.5%
18.3%
3D auto-refine
7.44 Å
Particle reextraction
(1.07 Å/px)
3D auto-refine with mask
CryoSPARC
Non-uniform refinement
4.28 Å
3.54 Å
DeepEMhancer
180°
Out
SLC19A1
5-MTHF
N
C
In
b
Elevation
Azimuth
# of images
c
GSFSC Resolution: 3.54Å
No Mask (4Å)
Loose (3.6Å)
Tight (3.5Å)
Corrected (3.5Å)
1/Resolution (1/Å)
d
6.0
4.5
3.0
e
Fourier Shell Correlation
4.08 Å
1/Resolution (1/Å)
f
TM1
TM2
TM3
TM4
TM5
TM6
TM7
TM8
TM9
TM10
TM11
TM12

Supplementary Fig. S4 Cryo-EM data processing of the 5-MTHF-bound SLC19A1 dataset. **a** Work flow of the data processing. **b** Orientation distribution of the particles used in final reconstruction. **c** FSC curves between two half maps. **d** Local resolution of the cryo-EM map. **e** FSC curve calculated between cryo-EM map and structural model. **f** Close-up view of the cryo-EM densities and fitted atomic models for representative regions of the structure.

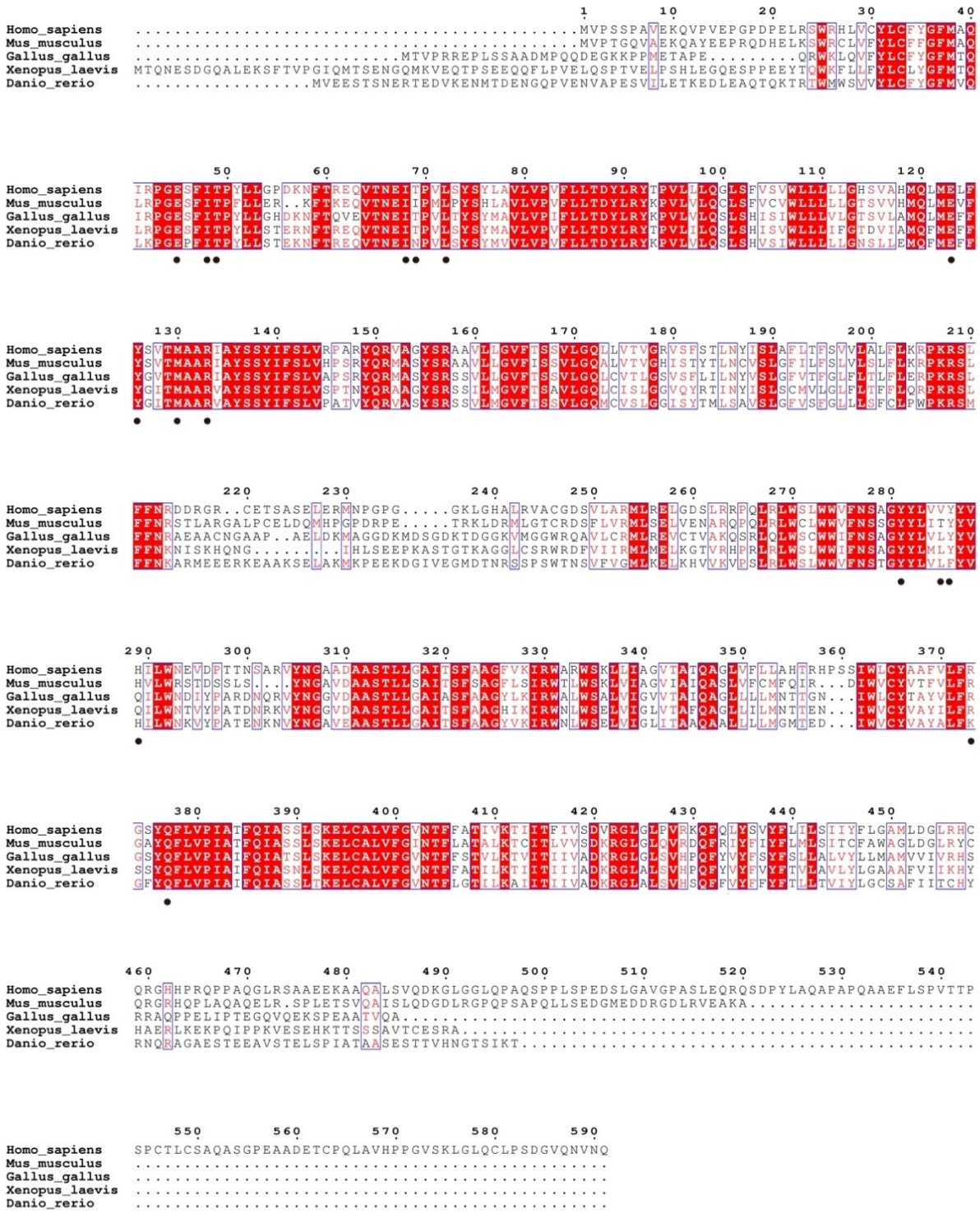

Supplementary Fig. S5 Sequence alignment of SLC19A1 among several representative species.

The residues participating into substrate binding are denoted by black dots.

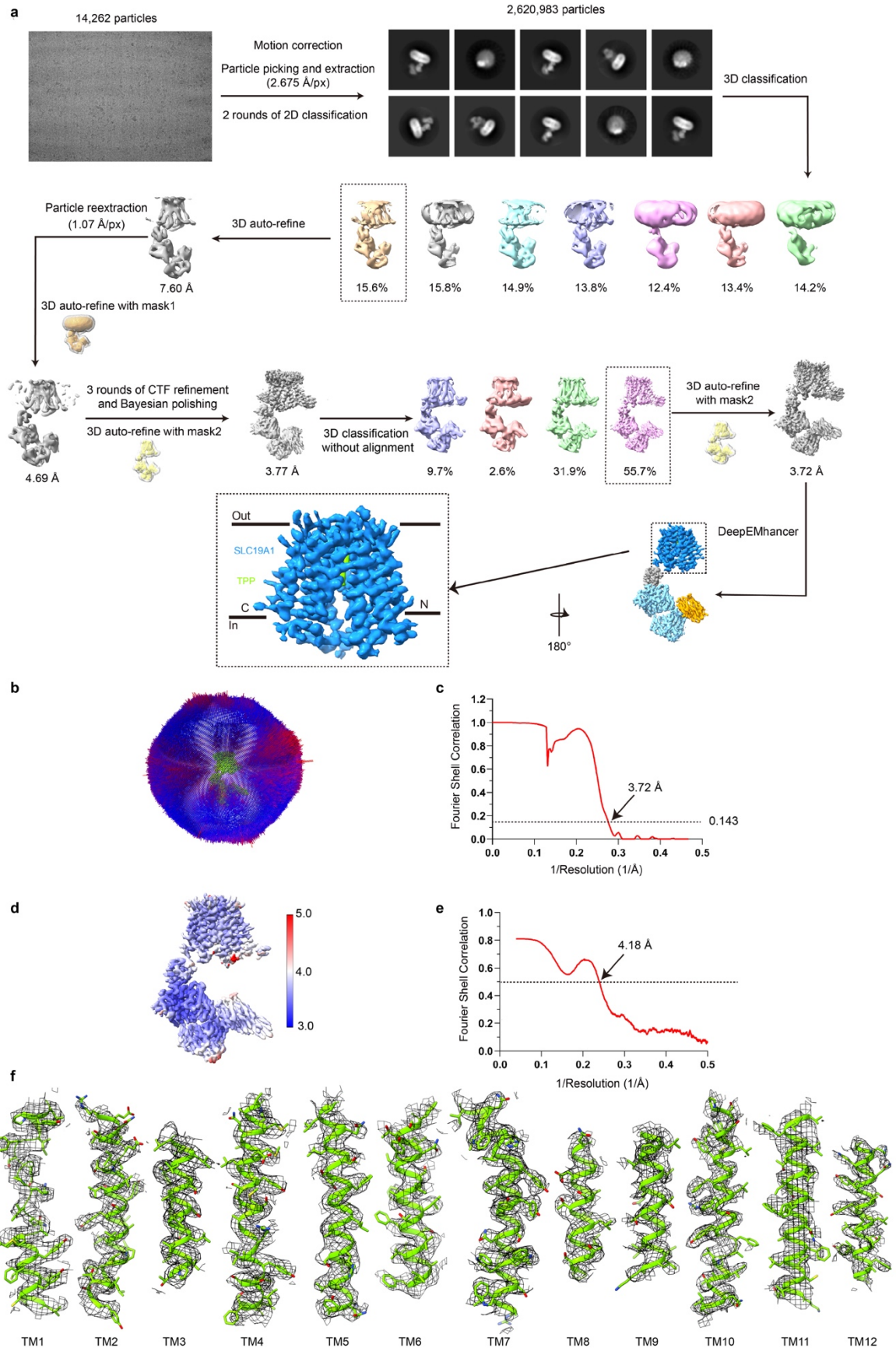
a
14,262 particles
Motion correction
Particle picking and extraction
(2.675 Å/px)
2 rounds of 2D classification
2,620,983 particles
3D classification
15.6%
15.8%
14.9%
13.8%
12.4%
13.4%
14.2%
3D auto-refine
Particle reextraction
(1.07 Å/px)
7.60 Å
3D auto-refine with mask1
4.69 Å
3 rounds of CTF refinement
and Bayesian polishing
3D auto-refine with mask2
3.77 Å
3D classification
without alignment
9.7%
2.6%
31.9%
55.7%
3D auto-refine
with mask2
3.72 Å
DeepEMhancer
Out
SLC19A1
TPP
C
N
In
180°
b
c
Fourier Shell Correlation
3.72 Å
0.143
1/Resolution (1/Å)
d
5.0
4.0
3.0
e
Fourier Shell Correlation
4.18 Å
1/Resolution (1/Å)
f
TM1
TM2
TM3
TM4
TM5
TM6
TM7
TM8
TM9
TM10
TM11
TM12

Supplementary Fig. S6 Cryo-EM data processing of the TPP-bound SLC19A1 dataset.

a Work flow of the data processing. **b** Orientation distribution of the particles used in final reconstruction. Red and higher cylinders represent more particles assigned to a particular orientation, while blue and shorter cylinders represent less. **c** FSC curve between two half maps. **d** Local resolution of the cryo-EM map. **e** FSC curve calculated between cryo-EM map and structural model. **f** Close-up view of the cryo-EM densities and fitted atomic models for representative regions of the structure.

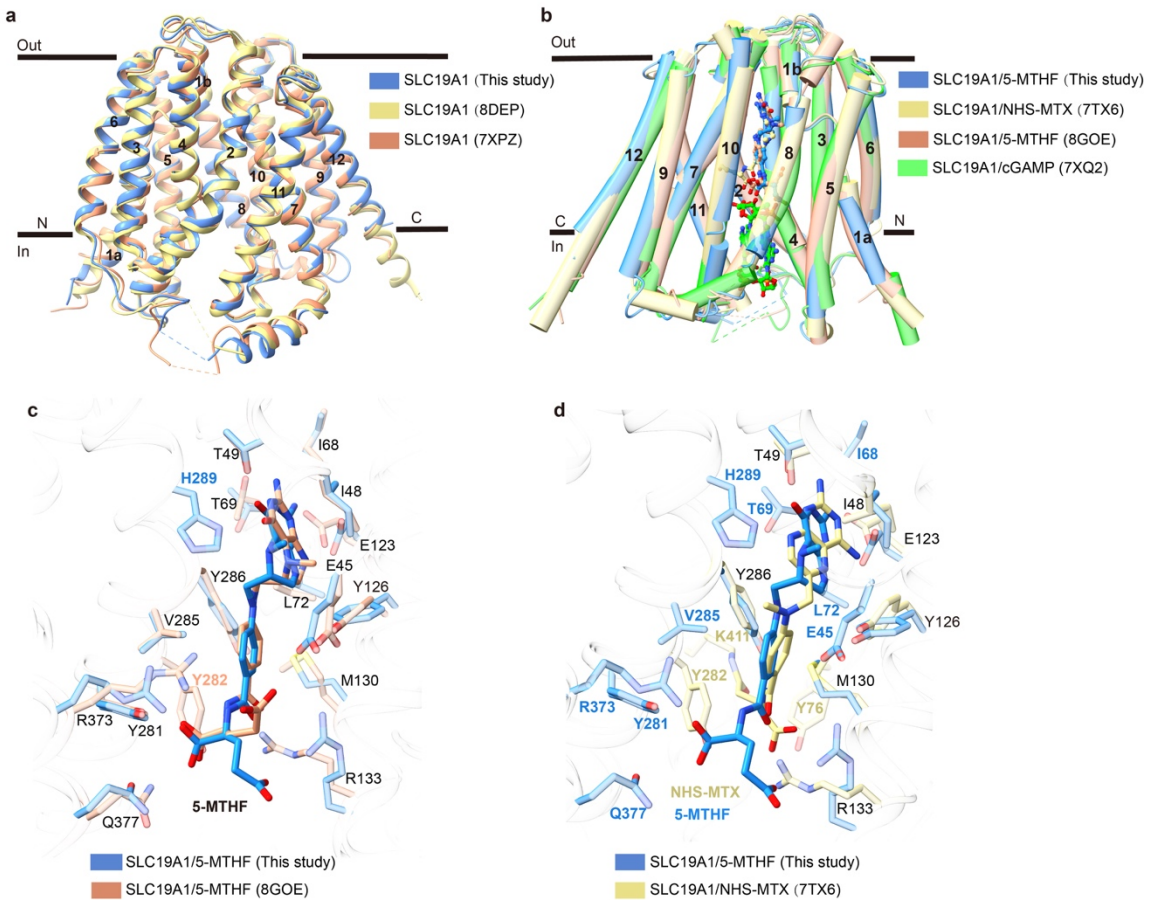

Supplementary Fig. S7 Superimposition of several SLC19A1 structures.

a Overlay of the apo SLC19A1 structures determined by three separate studies. The RMSDs between these structures are about 0.8 Å. **b** Overlay of the SLC19A1 structures in complexes with different substrates. The RMSDs between these structures are 0.8-1.0 Å. **c** Comparison of the binding details between SLC19A1 and 5-MTHF in our and reported structures. **d** Different conformations of the bound 5-MTHF and NHS-MTX. The residues involved in substrate binding are shown with side chains. Black labels represent the same residues verified in the two structures, while the colored labels represent the unique residues in each structure.

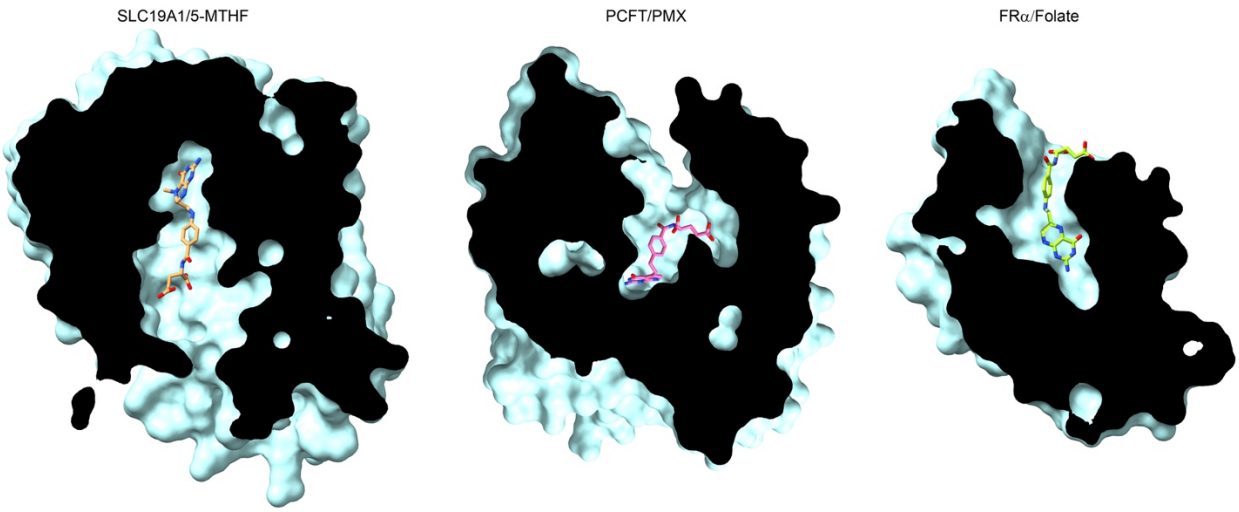

Supplementary Fig. S8 Structural comparison of the folate binding pockets in SLC19A1 (This study), PCFT (PDB: 7BC7), and FRα (PDB: 4LRH).

The three proteins are shown as surface presentation. Folate and analogs are shown as sticks.

Supplementary Table S1 Cryo-EM data collection, refinement, and validation statistics.

	Apo (EMD-34817) (PDB 8HII)	5-MTHF-bound (EMD-34818) (PDB 8HIJ)	TPP-bound (EMD-34819) (PDB 8HIK)
Data collection and processing			
Magnification	81,000	81,000	81,000
Voltage (kV)	300	300	300
Electron exposure (e^{-}/Å^2)	60	60	60
Defocus range (μm)	0.7-1.5	0.7-1.5	0.7-1.5
Pixel size (Å)	1.07	1.07	1.07
Symmetry imposed	C1	C1	C1
Initial particle images (no.)	3,104,540	1,802,524	4,144,030
Final particle images (no.)	268,975	206,075	229,158
Map resolution (Å)	3.57	3.54	3.72
FSC threshold	0.143	0.143	0.143
Map resolution range (Å)	2.9-12	2.9-15	3.2-12
Refinement			
Initial model used (PDB code)	6WW2	6WW2	6WW2
Model resolution (Å)	3.96	4.08	4.18
FSC threshold	0.5	0.5	0.5
Model resolution range (Å)	-	-	-
Map sharpening *B* factor (Å^2)	-	-	-
Model composition			
Non-hydrogen atoms	8,212	8,245	8,238
Protein residues	1,055	1,055	1,055
Ligands	-	1 (5-MTHF)	1 (TPP)
B factors (Å^2)			
Protein	66.65	96.48	70.07
Ligand	-	80.70	67.24
R.m.s. deviations			
Bond lengths (Å)	0.003	0.003	0.003
Bond angles (°)	0.790	0.727	0.776
Validation			
MolProbity score	1.51	1.52	1.61
Clashscore	3.48	3.77	4.75
Poor rotamers (%)	0.00	0.00	0.00
Ramachandran plot			
Favored (%)	94.64	94.83	94.74
Allowed (%)	5.36	5.17	5.26
Disallowed (%)	0.00	0.00	0.00